Electronic Supplementary Material (ESI) for RSC Advances.
This journal is © The Royal Society of Chemistry 2017

Electronic supplementary information

Engineering π-π Interactions for Enhanced Photoluminescent Properties: Unique Discrete Dimeric Packing of Perylene Diimides

*Yu Shao,[1, #] Guang-Zhong Yin,[2, #] Xiangkui Ren,[3] Xinlin Zhang,[1] Jing Wang,[4] Kai Guo,[5] Xiaopeng Li,[6] Chrys Wesdemiotis,[5] Wen-Bin Zhang,[2] Shuguang Yang,[1] Meifang Zhu,[1, *] and Bin Sun[1, *]*

[1] State Key Laboratory for Modification of Chemical Fibers and Polymer Materials, College of Materials Science and Engineering, Donghua University, 201620, Shanghai, P. R. China

[2] Key Laboratory of Polymer Chemistry & Physics of Ministry of Education, Center for Soft Matter Science and Engineering, College of Chemistry and Molecular Engineering, Peking University, Beijing 100871, P. R. China

[3] School of Chemical Engineering and Technology, Tianjin University, Tianjin 300072, China

[4] South China Advanced Institute of Soft Matter Science and Technology, South China University of Science and Technology, Guangzhou 510640, P. R. China

[5] Department of Chemistry, The University of Akron, Akron, OH 44325-3909, U.S.A.

[6] Department of Chemistry, University of South Florida, 4202 East Fowler Ave, Tampa, Florida 33620

#: These authors contribute equally to the work.

Experimental Section

Materials and Sample Preparations. POSS-PDI-POSS conjugates **1** and **2** and compound **3** were synthesized according to literature procedures.[S1-S3] Small, thin, belt-shaped crystals were prepared via different crystal growth procedures for structural determination. A solution (typically, 0.01 (w/v) % in tetrahydrofuran, or THF) was cast on carbon-coated mica surfaces and the sample was allowed to crystalize with slow evaporation in a controlled atmosphere saturated with THF, a method called "slow evaporation induced crystallization". After that, the single crystals were collected on copper grids for transmission electron microscopy (TEM). Larger crystals were grown by slow-diffusion of the poor solvent (e.g. methanol) into the solution in a good solvent (e.g. chloroform), a method called "slow diffusion induced crystallization". The process was carried out in a sealed test tube with the dense good solvent solution as the bottom layer and the light poor solvent as the upper layer, and the mixed solvent as the middle layer. The solubility of PDI decreases as the good and poor solvent slowly diffuse into each other. The red belt-shaped single crystals were formed at the interface and collected for 1D wide angle X-ray diffraction (WAXD), four element single crystal X-ray diffraction, polarized light microscopy (PLM), UV-vis absorption and photoluminence experiments.

Instrument and Characterization. Ultra-violet and visible (UV-Vis) spectra were recorded on a Lambda 35 (Perkin Elmer) spectrophotometer. The excitation and emission spectra of the samples were recorded on a FP-6600 steady-state fluorescence spectrophotometer (analysis range 200-800 nm with a resolution of 1 nm). The solution fluorescent quantum yields were measured using

Rhodamine 6G in ethanol solution as a standard with a known quantum yield of 86% [S4] and the calculations were done according to Eq. (1):

$$\phi_{\text{unk}} = \phi_{std}(I_{unk} / A_{unk})(A_{std} / I_{std})(\eta_{unk} / \eta_{std})^2 \qquad \text{Eq. (1)}$$

where the subscript *unk* and *std* represents the sample and the standard, respectively; Φ is the fluorescent quantum yield; I is the integrated emission intensity; A is the absorbance at the excitation wavelength; and η is the refractive index of the corresponding solution.

Solid-state steady-state fluorescence spectra and fluorescence quantum yield measurements were obtained on a JASCO FP-6600 spectrofluorimeter equipped with a 60mm diameter integrating sphere accessory and corresponding software. Sample crystals and powders were placed in a 10 mm diameter holder with a quartz window. The measured spectra were blank corrected by performing measurements for the reflectance standard (Al_2O_3), with the sample emission spectrum measured under the same conditions. The excitation wavelength can be chosen in the 350-750 nm range of the spectrum.

1D WAXD powder pattern was taken with a Rigaku MultiFlex 2 kW tube-anode X-ray (Cu Kα radiation) generator coupled to a diffractometer at room temperature. The samples were scanned with 1°/min scanning rate. The peak positions were calibrated using silicon powder in the high-angle region (> 15°) and silver behenate in the low-angle region (< 15°).

Crystals of **1** were coated in paratone oil, mounted on a CryoLoop™ and placed on a goniometer under a stream of nitrogen. X-ray data were collected using a Bruker Apex CCD diffractometer with graphite-monochromated Mo *K*α radiation (λ = 0.71073 Å). The frames were integrated with the Bruker SAINT software package using a narrow-frame algorithm. Data were corrected for

absorption effects using the multi-scan method (SADABS). The structure was solved and refined using the Bruker SHELXTL Software Package. The structure was determined by full-matrix least-squares refinement of F^2 and the selection of appropriate atoms from the generated difference map. Crystal data for **1**: $C_{86}H_{146}N_2O_{28}Si_{16}$, M = 2105.49, triclinic, a = 1.14 nm, b = 2.09 nm, c = 2.31 nm, α = 89.9°, β = 81.9°, γ = 82.3°, V = 5422.2 Å^3, T = 100 K, space group $P\bar{1}$, Z = 2, $\mu_{(MoK\alpha)}$ = 0.258 mm^{-1}, 38802 reflections measured, 18990 independent reflections (R_{int} = 0.0589). The final R_1 values were 0.0690 ($I > 2\sigma(I)$). The final $wR(F^2)$ values were 0.1720 ($I > 2\sigma(I)$). The final R_1 values were 0.1334 (all data). The final $wR(F^2)$ values were 0.1974 (all data). The goodness of fit on F^2 was 0.925.

A Philips Tecnai 12 TEM (accelerating voltage of 120 kV) were used to carry out selected-area electron diffraction along different crystal orientations on a tilting stage to determine the crystal structure parameters. The *d*-spacing was calibrated using a TlCl standard. The tilting angle was defined as positive if the tilting direction was clockwise and negative if counter-clockwise. Crystal morphology was observed under an Olympus HB-2 system in polarized light microscopy (PLM) mode.

Electrospray ionization (ESI) mass spectra were obtained on a Waters Synapt HDMS quadrupole/time-of-flight (Q/ToF) tandem mass spectrometer equipped with traveling wave ion mobility (TWIM) capability as described previously.[32] The following parameters were used in the TWIM-MS experiments: ESI capillary voltage, 3.5 kV; sample cone voltage, 35 V; extraction cone voltage, 3.2 V; desolvation gas flow, 800 L/h (N2); trap collision energy (CE), 6 eV; transfer CE, 4 eV; trap gas flow, 1.5 mL/min (Ar); IM gas flow, 22.7 mL/min (N2); sample flow rate, 10 μL/min;

source temperature, 30 °C; desolvation temperature, 40 °C; IM traveling wave velocity, 380 m/s; IM traveling wave height, 15 V. In the tandem mass spectrometry (MS/MS) experiments, argon was used as the collision gas and the trap CE was varied from 6 to 45 eV to cause fragmentation. The sprayed solution was prepared by dissolving ~ 1 mg of sample in 1 mL of a MeOH/THF (v/v = 1:3) mixture and adding 5 μL of 10 mg/mL NaTFA in THF as the cationizing agent.

Results and Discussions on Structure Determination by SAED in TEM

As described earlier, single crystalline nano-belts can also be grown by the slow evaporation induced crystallization method. Do the two methods (namely "slow evaporation induced crystallization" and "slow diffusion induced crystallization") generate crystals with the same structure? In addition to the WAXD experiments, we also carried out Selected Area Electron Diffraction (SAED) experiments in TEM. Fig. S6a shows part of the single crystal morphology observed under TEM, and Fig. S6b is the corresponding SAED pattern. As shown in Fig. S6b, the reciprocal angle between the two reciprocal axes is 97.7°, which is consistent with the (180º - γ) angle obtained from the WAXD crystallographic analyses. Therefore, this must be the γ^* angle, and the SAED pattern in Fig. S6b must be the [001] zone ED pattern. Along the b^*-axis in the SAED pattern, there are six diffraction spots and their *d*-spacing values follow integral ratios with respect to each other. The triclinic unit cell is primitive and there are no extinction rules for all the diffractions, so that the observed diffraction spots are the (010), (020), (030), (040), (050), and (060) diffractions with a *d*-spacing of 2.09 nm for the (010) diffraction. Along the a^*-axis in the SAED pattern, three layers of diffraction spots can be detected. The spot corresponding to the smallest 2θ angle on the first layer diffraction can be assigned as the (100) diffraction with a *d*-spacing of 1.14 nm. Therefore, the *ab*-plane of the

2D unit cell dimensions agrees well with the structure determined by the WAXD crystallographic analyses.

Further proof of the crystal structure was obtained from a series of SAED experiments on tilted samples. Fig. S6c shows a SAED pattern that was obtained by tilting the sample 42° clock-wise around the *a**-axis of the [001] zone ED pattern. On the zero diffraction layer along the *a**-axis, the diffraction pattern and the intensity ratios are identical to those shown in Fig. S6b, since the tilting is along the *a**-axis. However, on the first and second diffraction layers parallel to the *a**-axis, the diffraction pattern and intensity ratio are different from those in Fig. S6b, which is direct evidence that this is the ED pattern from a different diffraction zone. These diffraction spots on the first and second diffraction layers parallel to the a^*-axis have the *d*-spacings and angles in good agreements with those calculated utilizing the [011] zone pattern based on result of the WAXD crystallographic analyses. Therefore, the ED pattern in Fig. S6c is taken along the [011] zone. Similarly, the [0-11] zone ED pattern can be obtained by a counterclockwise tilting of the sample by 42° around the *a**-axis (Fig. S6d, the diffraction spots are weak due to the electron-beam damage in the sample, yet the relative intensity can be recognized and associated with the simulated pattern, see Fig. S7). Based on these SAED experimental results, the crystallographic parameters of the unit cell determined by the WAXD crystallographic analyses were confirmed. The molecular packing model of Fig. 3 was then used to simulate ED patterns along different zones. A comparison between the experimental results from different zones (Fig. S6) and the simulated ED patterns (Fig. S7) generated by the crystal packing model provides a qualitative corroboration of the results. The nano-belts and the bulk crystals shall have the same molecular packing scheme.

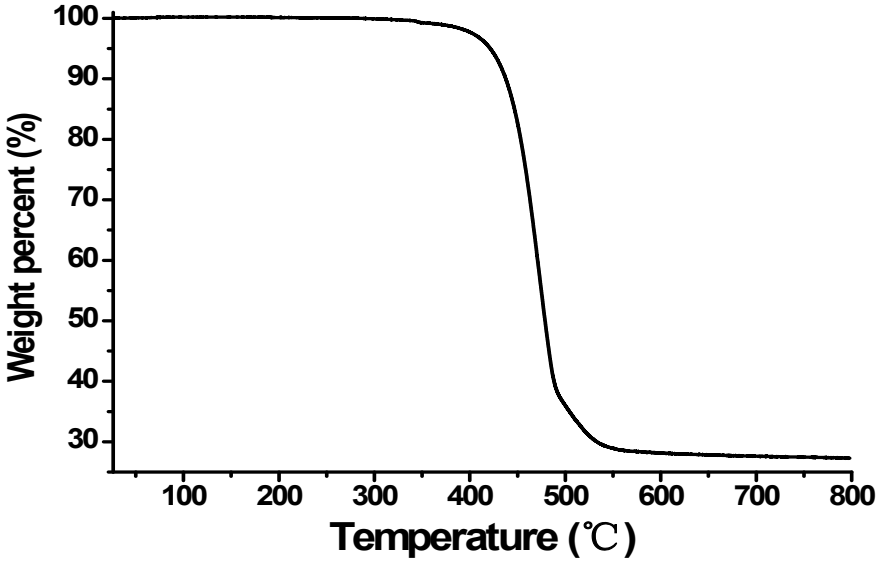

Fig. S1 TGA curve of compound **1**. The sample was heated under nitrogen from 30 °C to 800 °C at a scanning rate of 10 °C/min with TGA (Perkin-Elmer).

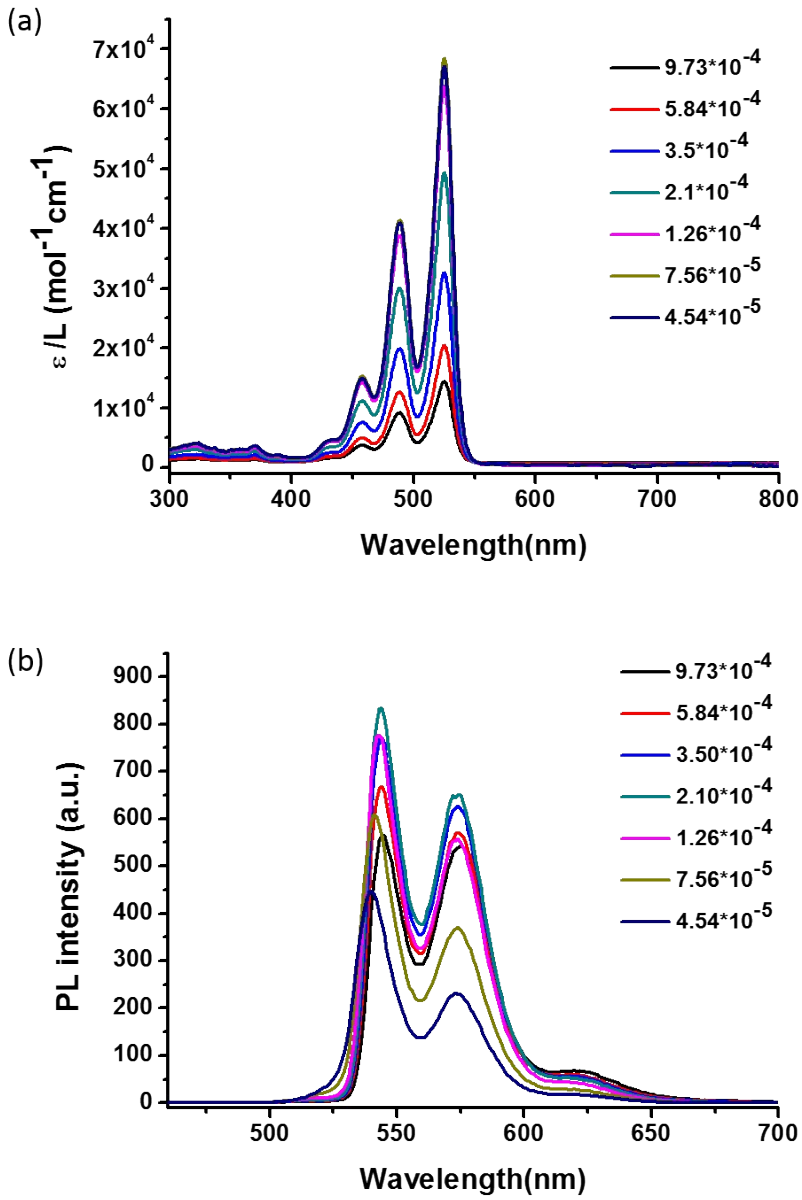

Fig. S2 Concentration-dependent UV-Vis absorption spectra and fluorescence emission spectra (λ_{ex}= 440 nm) of compound **3** in a single solvent, $CHCl_3$.

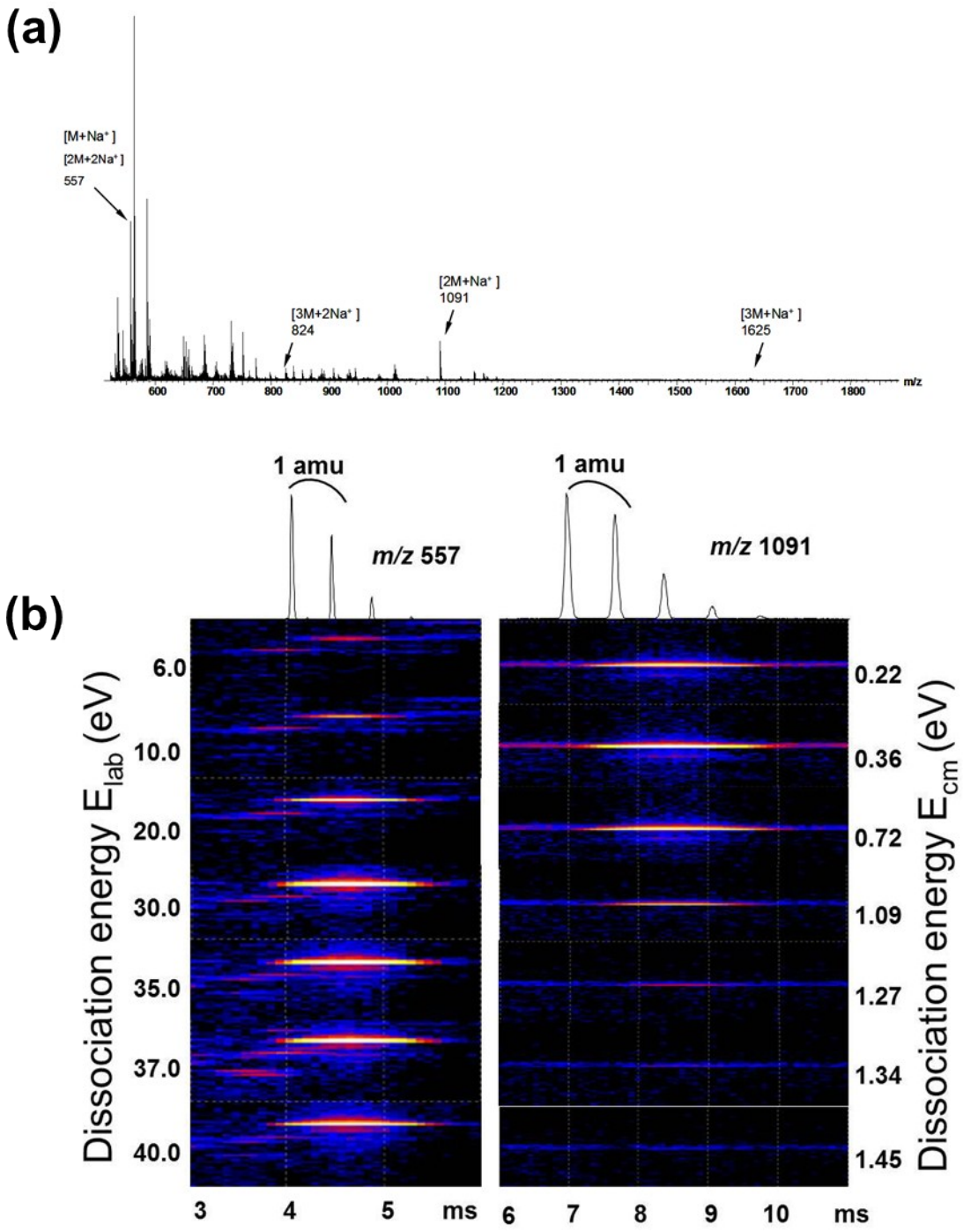

Fig. S3 (a) Full mass spectrum of compound **3** using NaTFA for cationizing agent. (b) Two-dimensional ESI-TWIM-MS plot of compound **3** for *m/z* 1091 and 557 dissociated from precursor ions at *m/z* 1091. The brightness of the color represents the intensity of the peak. Precursor ions at *m/z* 1091 were isolated by the Q for subsequent gradient tandem mass spectrometry in a trap cell at collision energies ranging from 6 to 40 eV.

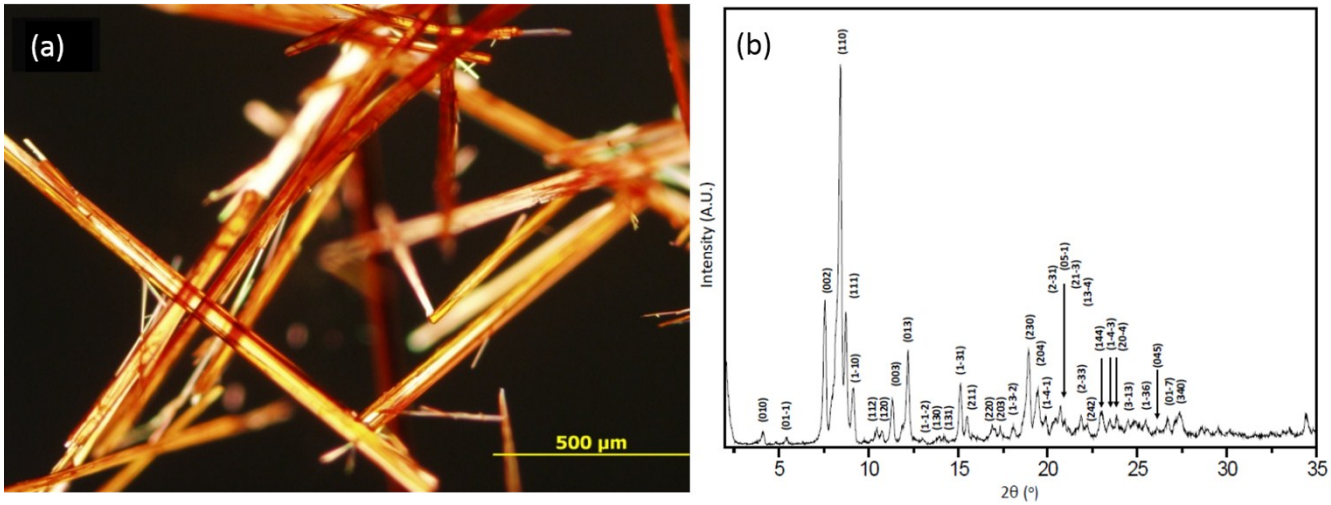

Fig. S4 (a) PLM image of the crystals of **1** and (b) 1D WAXD pattern of **1** at a scanning rate of 1°/min.

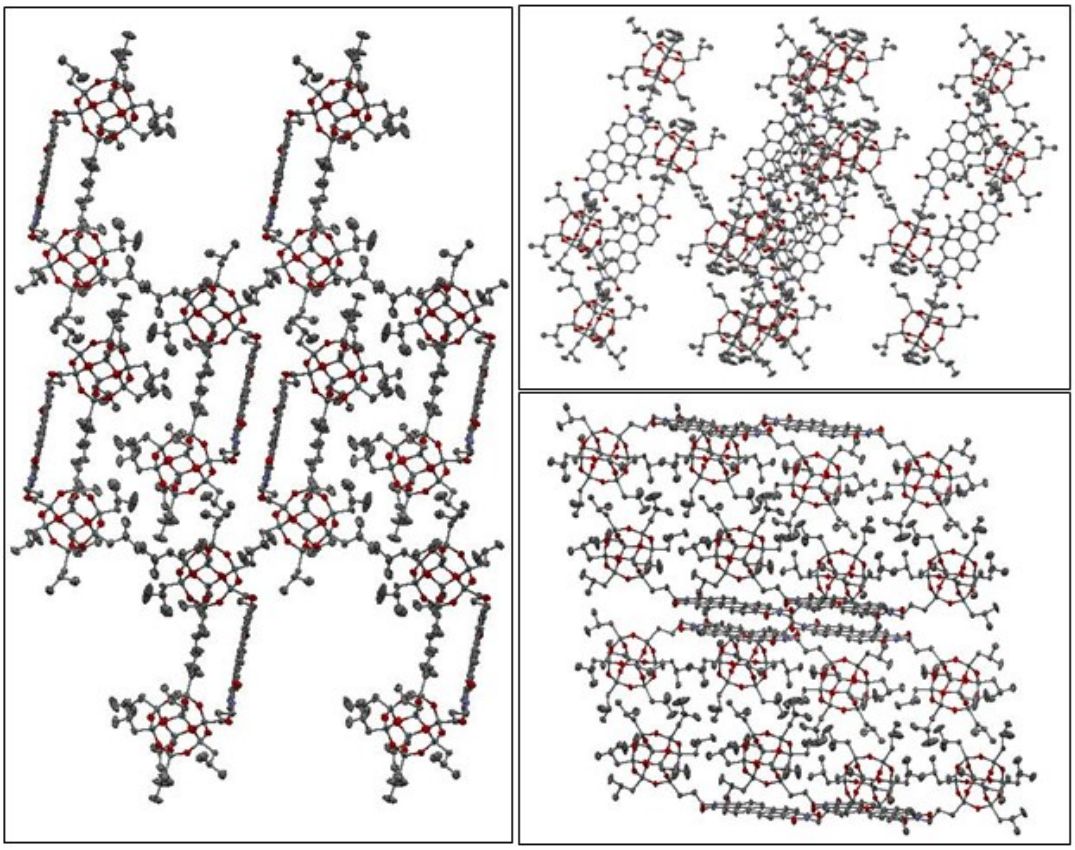

Fig. S5. Molecular packing in the crystal lattice of compound **1** on three different planes. Left: the *bc*-plane; Right upper: the *ac*-plane; Right bottom: the *ab*-plane. Each projection contains 4 unit cells along the projection plane.

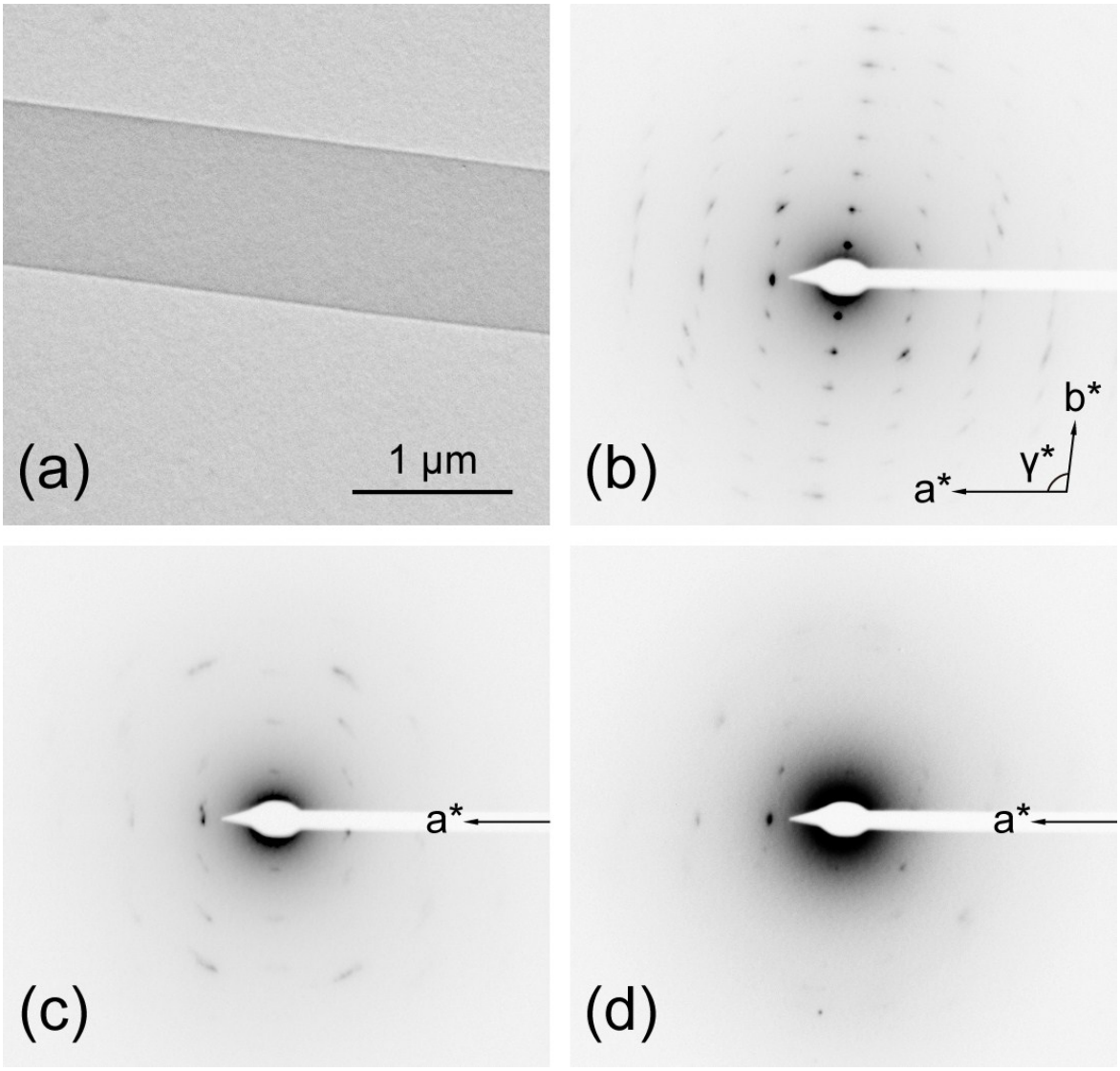

Fig. S6 (a) TEM bright field image of the single crystal nanobelt morphology of compound **1**; (b) SAED pattern along the [001] zone without tilting from the crystal in (a); (c) SAED pattern along the [011] zone; (d) SAED pattern along the [0-11] zone at room temperature. The patterns in (c) and (d) were obtained by tilting the sample 42° and -42° from [001] zone around c^*-axis, respectively.

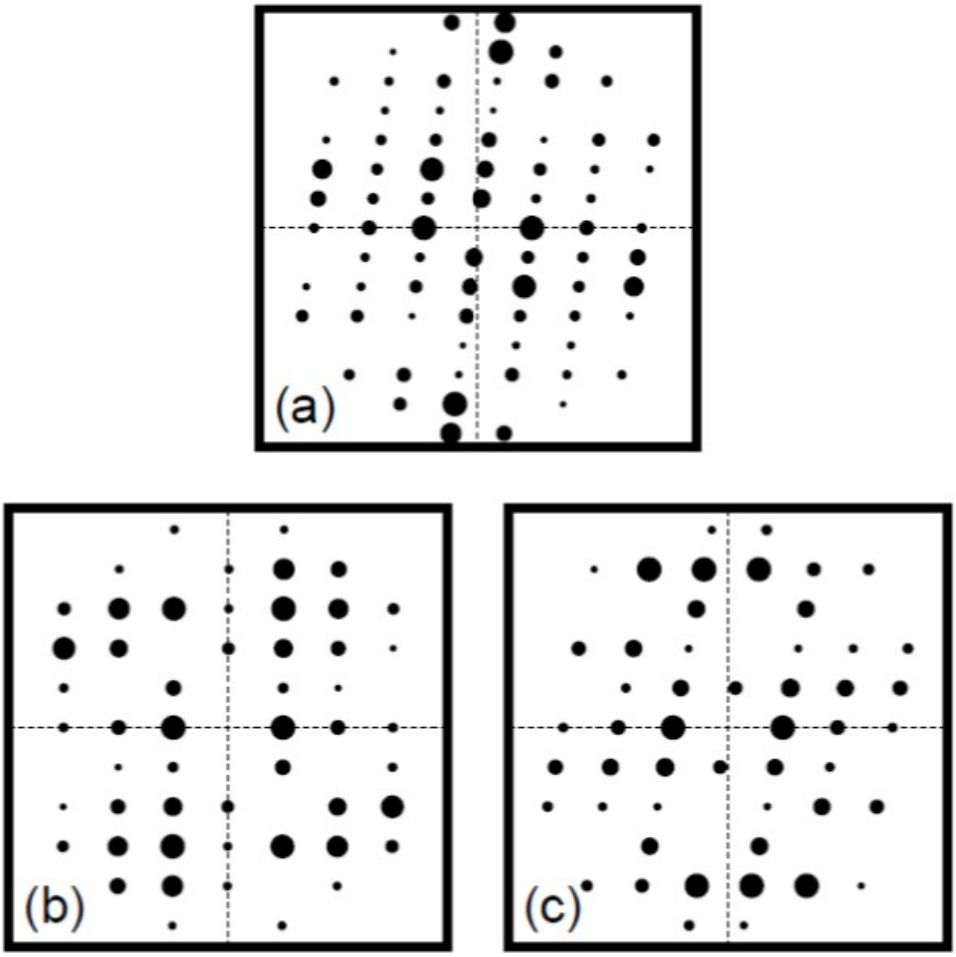

Fig. S7 Simulated SAED patterns of compound **1** from the [001] zone (a), [011] zone (b), and [0-11] zone (c), which agree with those of the experimental SAED (Fig. S6) diffraction patterns.

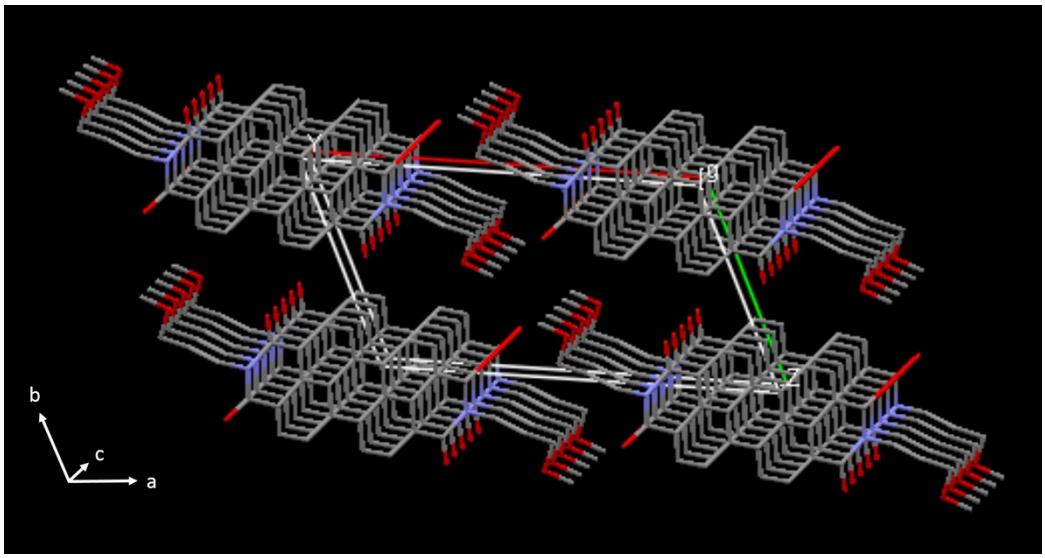

Fig. S8 Molecular packing of compound **3**. Four unit cells are shown and the π-π stacking appears to be continuous along the *c* axis.

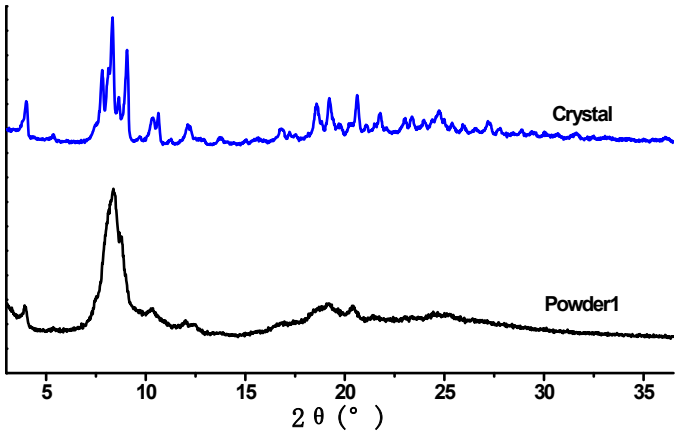

Fig. S9. The WAXD patterns of crystalline and precipitated powder sample of compound **1**.

Reference

(S1) X. K. Ren, B. Sun, C. C. Tsai, Y. F. Tu, S. W. Leng, K. X. Li, Z. Kang, M. V. H. Ryan, X. P. Li, M. F. Zhu, C. Wesdemiotis, W. B. Zhang, S. Z. D. Cheng, *J. Phys. Chem. B* 2010, **114**, 4802-4810.

(S2) H. Langhals, *Heterocycles* 1995, **40**, 477-500.

(S3) K. Balakrishnan, A. Datar, T. Naddo, J. L. Huang, R. Oitker, M. Yen, J. C. Zhao, L. Zang, *J. Am. Chem. Soc.* 2006, **128**, 7390-7398.

(S4) J. Olmsted, *J. Phys. Chem.* 1979, **83**, 2581-2584.